Analytica Chimica Acta 1044 (2018) 181–190

Contents lists available at ScienceDirect

Analytica Chimica Acta

journal homepage: www.elsevier.com/locate/aca

Heterogeneity assessment of antibody-derived therapeutics at the intact and middle-up level by low-flow sheathless capillary electrophoresis-mass spectrometry

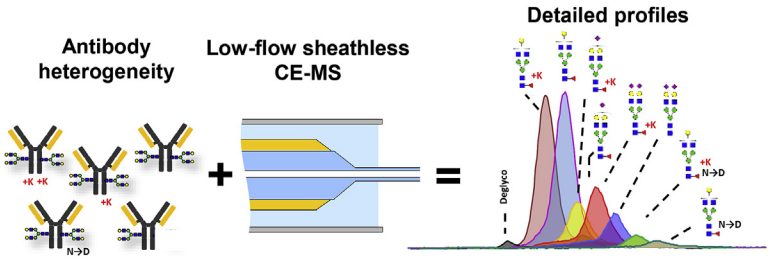
Rob Haselberg [a], Thomas De Vijlder [b], Raimond Heukers [c], Martine J. Smit [c], Edwin P. Romijn [b], Govert W. Somsen [a, *], Elena Domínguez-Vega [a, 1]

[a] Division of BioAnalytical Chemistry, Department of Chemistry and Pharmaceutical Sciences, Vrije Universiteit Amsterdam, de Boelelaan 1085, 1081 HV, Amsterdam, The Netherlands
[b] Pharmaceutical Development and Manufacturing Sciences, Janssen Research and Development, Turnhoutseweg 30, 2340, Beerse, Belgium
[c] Division of Medicinal Chemistry, Faculty of Sciences, Vrije Universiteit Amsterdam, de Boelelaan 1085, 1081 HV, Amsterdam, The Netherlands

HIGHLIGHTS

- Low-flow CE-MS allows detailed characterization of heterogeneous antibodies.
- Applicability is demonstrated for nanobody and mAb products.
- Isomeric nanobody variants and fragments were efficiently resolved and assigned.
- CE-MS of intact mAb products reveals presence of singly glycosylated and clipped forms.
- Middle-up CE-MS of provides in-deep and detailed characterization of mAb microheterogeneity.

GRAPHICAL ABSTRACT



ARTICLE INFO

Article history:
Received 12 May 2018
Received in revised form
9 August 2018
Accepted 12 August 2018
Available online 15 August 2018

Keywords:
Sheathless CE-MS
Low-flow CE
Monoclonal antibodies
Nanobodies
Intact protein analysis
Middle-up analysis

ABSTRACT

Antibody-based pharmaceuticals often encompass a complex structural heterogeneity requiring enhanced analytical methods for reliable characterization of variants and degradation products. We have explored the capabilities of low-flow sheathless capillary electrophoresis-mass spectrometry (CE-MS) for the high-resolution and sensitive profiling of antibody therapeutics. Near-zero electroosmotic flow was achieved by employing a novel neutral capillary coating that also prevents protein adsorption. CE-MS analysis of intact model proteins using an acidic background electrolyte demonstrated satisfactory performance, with overall migration-time RSDs below 2.2% from three different capillaries tested. For system evaluation, three nanobody preparations, including mono- and bivalent forms, and three monoclonal antibodies (mAbs) were analyzed. Intact nanobodies were resolved from their degradation products, which could be assigned to deamidated, cleaved, and truncated forms at the C-terminal tag. Excellent resolution of isomeric deamidated products was obtained. The mAbs were analyzed intact and after digestion by the endoproteinase IdeS (middle-up approach). CE-MS of intact mAbs provided resolution of clipped species (e.g. light chain and light chain-heavy chain fragments) from the native protein. Moreover, glycoforms containing sialic acids were resolved from their non-sialylated counterparts. For IdeS-digested, F (ab)$_2$ and Fc/2 portions where efficiently resolved for the three mAbs. Whereas the

* Corresponding author.
E-mail address: g.w.somsen@vu.nl (G.W. Somsen).
[1] Current address, Center for Proteomics and Metabolomics, Leiden University Medical Center, Postbus 9600, 2300 RC Leiden, The Netherlands.

https://doi.org/10.1016/j.aca.2018.08.024
0003-2670/© 2018 The Authors. Published by Elsevier B.V. This is an open access article under the CC BY license (http://creativecommons.org/licenses/by/4.0/).

migration time of the Fc/2 fragments was fairly similar, the migration time of the F $(ab)_2$ part was strongly varied among the mAbs. For all mAbs, separation of Fc/2 charge variants - including sialylated glycoforms and other post-translational modifications, such as loss of C-terminal lysine or asparagine deamidation - was achieved. This allowed a detailed and reliable assessment of the Fc/2 heterogeneity (18–33 proteoforms) of the three analyzed mAbs.

© 2018 The Authors. Published by Elsevier B.V. This is an open access article under the CC BY license (http://creativecommons.org/licenses/by/4.0/).

1. Introduction

Significant advances in therapeutic-protein development over the last decades have resulted in the production of a variety of antibody-derived therapeutics and fusion proteins. Since the introduction of the first immunoglobulin G (IgG) for therapeutic purposes [1], nearly fifty antibody-based pharmaceuticals have been approved for clinical use and are available on the market [2], and many are currently in development. Today, monoclonal antibodies (mAbs) represent a major class of biopharmaceuticals providing efficacious therapies for severe and life-threatening diseases, and generating high revenues for the pharmaceutical industry. The success of mAbs mainly relies on their high specificity and limited side effects [3]. Still, IgG-type mAbs are large heteromultimeric protein species, which require complex manufacturing processes and entail high production costs [4,5]. Most mAbs are expressed in mammalian cell cultures and may undergo various post-translational modifications (PTMs), resulting in an intrinsic structural heterogeneity. Monitoring of mAb variants and potential degradation products by adequate analytical techniques is essential to ensure quality, efficacy and production consistency.

Over the last years, there is a growing interest in the potential therapeutic use of so-called nanobodies as possible alternatives for mAbs. Nanobodies are single-domain antibody fragments derived from the variable domains of heavy-chain-only antibodies found in members of the *Camelidae* family [5,6]. Nanobodies are relatively small proteins (12–15 kDa) exhibiting a binding capacity and specificity similar to mAbs, while exhibiting higher chemical stability. Moreover, the relatively straightforward generation of nanobody constructs using, for example, short peptide linkers, provides opportunities for developing therapeutics with improved potency and/or multiple specificities [5,6]. Nanobodies are expressed in and isolated from *E. coli* and may show production variability (e.g. deamidated forms or pyroglutamate formation), degradation products and size variants, which obviously have to be characterized using proper analytics.

Mass spectrometry (MS) has become a primary technique for antibody characterization, in particular in early stage development [7–9]. MS can provide highly useful data on protein integrity, purity and heterogeneity. Depending on the protein information required, MS has been used for the analysis of intact protein pharmaceuticals, of the peptides obtained after their enzymatic digestion, or of their glycans after release. Intact protein (and top-down) analysis may be of particular benefit for biopharmaceutical analysis as it offers a general picture of the heterogeneity of the protein population, while inducing minimal changes caused by sample treatment. Furthermore, analysis of proteins at the intact level provides information about the exact combination of multiple modifications, which cannot be revealed by merely bottom-up approaches [10,11]. MS analysis of intact mAbs (150 kDa) may be hampered by limited ionization efficiency and mass resolution. Applying a middle-up approach, the antibody of interest is treated with a specific protease (*e.g.* IdeS endoproteinase) or reducing agent (*e.g.* dithiothreitol) to produce large antibody subunits (25–50 kDa), thereby facilitating the MS-based assessment of the mAb microheterogeneity [7].

Heterogeneity analysis of biopharmaceuticals by direct MS remains a challenge as most therapeutic proteins represent mixtures of structurally highly related species. This means that for reliable characterization often a pre-separation is required to distinguish variants and detect subtle modifications. However, efficient separation of intact proteins under MS-compatible conditions is not straightforward. Capillary electrophoresis (CE) has the intrinsic capacity to produce narrow peaks for proteins and shows great potential for the separation of protein variants and isoforms [12–15]. CE-MS of intact proteins, including profiling of pharmaceutical (glyco)proteins, has been demonstrated widely [12,13,16]. However, reports on the use of CE as a front-end separation technology prior to antibody characterization by MS have been quite scarce so far. Redman et al. used an integrated microfluidic CE device with a positively-charged channel-coating to prevent protein adsorption, for the MS-based characterization of intact mAbs [17] and antibody-drug conjugates [18]. C-terminal lysine, pyroglutamic acid and decarboxylation charge variants were partially resolved, whereas glycoforms of the analyzed mAbs were not separated, but some could be assigned in the deconvoluted mass spectra. Lately, the group of Neusüß reported on the MS identification of some charge variants of intact mAbs, which were separated by capillary isoelectric focusing (CIEF) [19] or CE employing non-volatile buffers [20] in a first dimension, and then on-line transferred to a MS-compatible CE system for interference-free MS detection. Haselberg et al. used sheath-liquid CE-MS for purity analysis of a nanobody targeting the epidermal growth factor receptor employing background electrolytes (BGEs) of medium and low pH in combination with negatively- and positively-charged capillary coatings, respectively [21,22].

In earlier work, our group has shown the usefulness of sheathless CE-MS employing a capillary with a neutral coating for glycoform profiling of intact therapeutic proteins in the 20–35 kDa range [12]. The near-zero electroosmotic flow yielded enhanced CE resolution of protein variants, while the nano-electrospray conditions provided the sensitivity to detect low-abundant glycoforms. Zhao et al. and Han et al. [23,24] used neutral linear polyacrylamide-coated capillaries in combination with a nanoflow sheath-liquid interface for CE-MS analysis of reduced and IdeS-digested mAbs. The antibody subunits could be separated, but further resolution and assignment of variants and glycoforms was not reported. Just recently, sheathless CE-MS of one mAb was described as part of a native MS study. A BGE of 20 mM ammonium acetate (pH 8.0) was used in combination with a commercial neutral polyacrylamide-coated capillary with a porous emitter tip. A mAb product that lost two light chains and the dimer of the corresponding light chains were separated from the native mAb by CE. Still, the predominant forms of the mAb, comprising doubly and singly glycosylated, and dimeric structures co-migrated with the native mAb. The identity of these species, including some glycoforms, was derived from the complex high-resolution mass spectrum recorded for the main peak.

The aim of the present work was to further explore the capabilities of low-flow sheathless CE-MS employing acidic BGEs for the characterization of antibody-type therapeutics. A new commercially-available neutrally-coated capillary was evaluated and used to achieve near-zero electroosmotic flow and to circumvent protein adsorption. Two monovalent nanobody preparations, Nb1 and Nb2 (each comprising a Myc-6xHis tag), and a bivalent construct (Nb1-35 GS-Nb1) of two Nb1 domains were analyzed to assess the performance of the low-flow CE-MS system for distinguishing nanobody production variants. Moreover, several mAbs exhibiting different levels of charge and glycosylation heterogeneity were analyzed by low-flow CE-MS using both intact and middle-up approaches in order to evaluate the mAb proteoform resolution.

2. Experimental

2.1. Chemicals

All reagents employed were of analytical grade. Ammonium hydroxide (25% solution) was obtained from Sigma Aldrich (Steinheim, Germany). Isopropanol, acetic acid and hydrogen chloride were obtained from Merck (Darmstadt, Germany). Lysozyme, cytochrome C, and ribonuclease A were kindly provided by Sciex (Brea, CA, USA). IdeS endoproteinase (immunoglobulin-degrading enzyme of Streptococcus pyogenes) was obtained from Genovis (Lund, Sweden). Commercially available pharmaceutical formulations of trastuzumab, infliximab and ustekinumab were used. Monovalent and bivalent nanobodies were produced as described in detail elsewhere [6]. Briefly, the nanobodies were C-terminally tagged with Myc-(EQKLISEEDLNG) and 6x-histidine tags, and were produced in BL21 E. *coli*. Periplasmic extracts were prepared by a freeze-thaw cycle of *E. coli* in phosphate buffered saline (PBS). Nanobodies were isolated from periplasmic extracts by ion-metal affinity chromatography using Ni-NTA agarose resin (Thermo Fischer Scientific, Waltham, MA, USA). Elution of the nanobodies from the Ni-NTA resin was performed with 250 mM imidazole in PBS. Finally, imidazole was removed via multiple dialysis steps against PBS using a 3.5 kDa MWCO SnakeSkin dialysis membrane (Thermo Fischer Scientific). Deionized water was obtained from a Milli-Q purification system (Millipore, Bedford, USA).

2.2. Sample preparation

A stock solution of cytochrome C, lysozyme, and ribonuclease A (1 mg/mL each) was prepared in water. Prior to injection the mixture was diluted 5 times in 10 mM ammonium acetate (pH 3.0). Nanobodies were diluted in 10 mM ammonium acetate (pH 3.0) to a final concentration of approximately 1 μM. The formulation buffer of the mAb samples was exchanged for water (for intact analysis) or PBS (for IdeS digestion) using Vivaspin 10 kDa MWCO filter tubes (Sartorius, Göttingen, Germany) applying six buffer exchange cycles using 15000 × g at 10 °C. Digestion of the antibodies was performed using the endoproteinase IdeS. For that purpose, 7.5 μL of the enzyme (67 units/μL) was added to 50 μL of a solution containing 5 mg/mL mAb in PBS. After that, 42.5 μL of water was added to obtain a final volume of 100 μL and the mixture was incubated at 37 °C for 30 min. After digestion, the samples were centrifuged three times against six volumes of water using Vivaspin 10 kDa MWCO filter tubes at 15000 × *g* and 10 °C. The sample residue was reconstituted in water to obtain a final concentration of 5 mg/mL. Prior to injection, all the samples were diluted in water to obtain the desired concentration (0.015–0.025 μg/μL for nanobody and 0.5 μg/μL for antibody samples).

2.3. Sheathless CE-MS

Sheathless integrated capillary electrophoresis electrospray ionization was carried out on a Sciex CESI 8000 instrument. The outlet of the separation capillary was placed in a grounded stainless-steel needle that could be positioned by an XYZ stage at the entrance of a Bruker maXis HD Ultra high resolution QTOF mass spectrometer (Bruker Daltonics, Bremen, Germany) equipped with a nano-electrospray ionization source. The mass spectrometer was operated in positive ionization mode using the following parameters: capillary voltage 1200 V, drying gas temperature 180 °C, drying gas flow rate 2 L min^{-1}. Mass spectra were collected in profile mode using a mass range of 500–3000 m/*z*. MS control and data acquisition and analysis were performed using QTOF control and data analysis software (Bruker Daltonics). Molecular mass determinations were performed using the 'Maximum Entropy' algorithm of the DataAnalysis software.

Pre-coated capillaries (length, 91 cm; 30 μm i. d.; 150 μm o. d.) with a porous tip were provided by Sciex (Neutral OptiMS Cartridge). The residual EOF was measured using pressure mediated CE for the 3 coating lots. The experiments were performed using nitromethane as neutral marker and 20 mM ammonium acetate pH 4.8 as BGE. The EOF values determined ranged from 1.27×10^{-06} to 1.01×10^{-06} $cm^2 \cdot V^{-1} \cdot S^{-1}$. The neutrally coated capillaries were conditioned according to the supplier specifications. Prior to first use, the capillary tip was inserted in a falcon tube containing 50 mL of water and the capillary was flushed for 5 min (100 psi, forward) with 0.1 M HCl, 10 min (100 psi, forward) with 50 mM ammonium acetate (pH 3.0) and 30 min (100 psi, forward) with water. After the last rinse, the capillary was equilibrated for 16–18 h to allow rehydration of the neutral coating. This step was performed only before the first injection or after capillary storage. Before each run, the capillary was flushed for 3 min at 100 psi with 0.1 M HCl followed by 10 min at 100 psi with the BGE. The conductive line was filled with the appropriate liquid by using reverse pressure during 3 min at 75 psi. For nanobody and middle-up mAb analysis, sample injection was carried out at 2.5 psi for 15 s. For intact mAb analysis, sample injection was at 2.5 psi for 10 s. The capillary temperature was set at 20 °C. For the test proteins and nanobodies, the background electrolytes (BGE) and conductive liquids were aqueous solutions of 50 mM ammonium acetate (pH 3.0) and 50 mM acetic acid, respectively. For intact mAbs, 10% acetic acid was employed as BGE as well as conductive liquid. For IdeS-digested mAbs, the BGE consisted of either 10% or 20% acetic acid, and 3% acetic acid was used as conductive liquid. At the end of each run, the voltage was lowered to 1 kV over 5 min.

3. Results and discussion

3.1. Basic performance of coated capillary

In previous work, we showed the potential of low-flow CE-MS for the analysis of intact therapeutic proteins, to enhance proteoform-resolution and increase sensitivity [12]. In the present work, the potential of low-flow CESI-MS for the characterization antibody-based therapeutics was investigated. To induce low-flow conditions, a novel neutral capillary coating was employed. This coating consists of a first, hydrophobic layer to protect siloxanes from hydrolysis, and a second layer of polyacrylamide providing a hydrophilic surface. With acidic BGEs, the electroosmotic flow (EOF) of the coated capillary was near-zero (1.27×10^{-06} to 1.01×10^{-06} $cm^2 \cdot V^{-1} \cdot S^{-1}$). In order to ensure stable electrospray formation during CE analysis, a small pressure of 0.5–1.5 psi was applied on the capillary inlet, inducing a flow rate of 5–15 nL/min. The suitability of the new neutral coating for intact protein analysis

was evaluated using a mixture of cytochrome C, lysozyme, and ribonuclease A (0.2 μg/μL each). Using a BGE of 50 mM ammonium acetate (pH 3.0), the three proteins showed narrow peaks with plate numbers of 100,000 and higher (Fig. S1 in Supplementary Information). The obtained protein resolution provided detection of several related impurities in the protein standards. For all test proteins, the mass spectra recorded in the peak apices showed a good quality with intensities for in the order of ~10^6 for the main charge state and low background noise, allowing the accurate assignment of the molecular masses of the respective proteins. The analytical performance of the coated capillaries was further evaluated by repeated CE-MS analysis of the protein test mixture using three individual capillaries (12 analyses per capillary). The RSDs for migration time and peak area were in the ranges 1.4–2.2% and 8.3–11% (n = 36), respectively, indicating the neutral coating permits intact protein analysis in a reproducible fashion.

3.2. Stability and purity assessment of nanobodies

To evaluate the potential of the low-flow CE-MS system for the purity and heterogeneity analysis of nanobodies, two nanobody preparations, Nb1 and Nb2, were assessed. Both Nb1 and Nb2 comprise of a non-glycosylated peptide chain of about 120 amino acids (approximately 15 kDa) and were designed to specifically bind extracellular domains of G-protein coupled receptors [6]. In addition, the bivalent construct Nb1-35 GS-Nb1, generated via genetic fusion of two Nb1 domains attached through a 35-mer peptide linker ((-GGGGS-)$_7$) [25], was analyzed.

A BGE of acetic acid, shown to be highly useful for intact protein analysis by CE-MS, was used for the analysis of the nanobodies [12,26] and the effect of the acetic acid concentration (50–250 mM) on the separation of the components of Nb2 was evaluated. Increasing the acetic acid concentration provided shorter protein migration times, accompanied by a decrease of protein peak resolution. Adjusting the pH of the BGE from 3.0 to 4.0 did not affect protein resolution, but resulted in a decrease of protein signal intensity. A significant increase of peak resolution was obtained by minimizing the pressure applied to the inlet capillary during the separation (Fig. S2). The minimum pressure at which a stable ESI signal was obtained appeared to be 0.5 psi, providing an overall flow rate of 5 nL/min. A BGE of 50 mM acetic acid (pH 3.0), a separation voltage of 30 kV, and a capillary inlet pressure of 0.5 psi were selected for the further CE-MS analysis of the nanobody samples.

CE-MS analysis of the monovalent Nb1 sample resulted in two partially separated peaks migrating at 12.0 and 12.5 min (Fig. 1A) with measured molecular masses of 14590.97 and 14591.90 Da, respectively (Table 1). The mass observed for the first migrating compound agrees with the theoretical mass of Nb1. The second peak, which had an area of about 50% relative to peak 1, was assigned to a deamidated form of Nb1. Deamidation is a common protein PTM that generally involves the conversion of an asparagine residue to aspartic acid, causing a small change of protein molecular mass (+0.984 Da) but a significant reduction of protein pI. The latter allows CE separation of the deamidated form from the native protein.

Low-flow sheathless CE-MS of the bivalent Nb1 construct (Nb1-35 GS-Nb1) yielded a main peak at 13.3 min (peak 4 in Fig. 1B), which could be assigned to the intact conjugate (deconvoluted mass, 28835.74 Da; Table 1). The peak migrating closely after the main peak (no. 5) showed a mass difference of +0.93 Da with respect to the native Nb1-35 GS-Nb1, indicating considerable deamidation (as for Nb1). Three minor peaks (no. 1–3) were observed migrating before the main peak (Fig. 1B; Table 1). Based on acquired deconvoluted masses, peaks 1 and 2 could be assigned to the monovalent Nb1 and its deamidated form, respectively. Peak 3 (deconvoluted mass, 15527.70 Da) may correspond to an Nb1 molecule carrying a fragment of the 35 GS linker.

The result of low-flow sheathless CE-MS analysis of the Nb2 nanobody preparation is depicted in Fig. 1C, indicating a large sample heterogeneity. Up to 22 peaks were observed between 12 and 17 min. Table 2 lists the deconvoluted masses derived from the mass spectra detected in the apices of the peaks, and the provisional assignments of these masses to possible structures. Peak 2 could be assigned to native Nb2, while the other peaks appeared to originate from products of truncation and/or deamidation of Nb2. Peaks 12–22 correspond to truncated Nb2 forms resulting from a loss of 6–18 amino acids at the C-terminus side, which corresponds to the C-terminal Myc-His tag of the nanobody. These C-terminal truncations correlate well with the corresponding peptide fragments (peaks 1, 4, 5, 8, 9 and 11) that were detected at shorter migration times. The truncations observed with this nanobody might be a result of non-specific digestion of the Myc tag by residual proteases in the sample, which would also indicate a higher stability of the nanobody portion as compared to the tag.

Next to Nb2 and its fragments, a number of deamidated forms were observed in the CE-MS profile (Table 2). Interestingly, several isomeric deamidated species were separated by CE and assigned. For example, the extracted-ion electropherogram obtained for the C-terminal fragment E130-H142 (extraction width, ± 0.5 m/z) revealed three base-line separated peaks (Fig. 2A top). The mass of the first peak (deconvoluted mass, 1639.79 Da) correlated well with

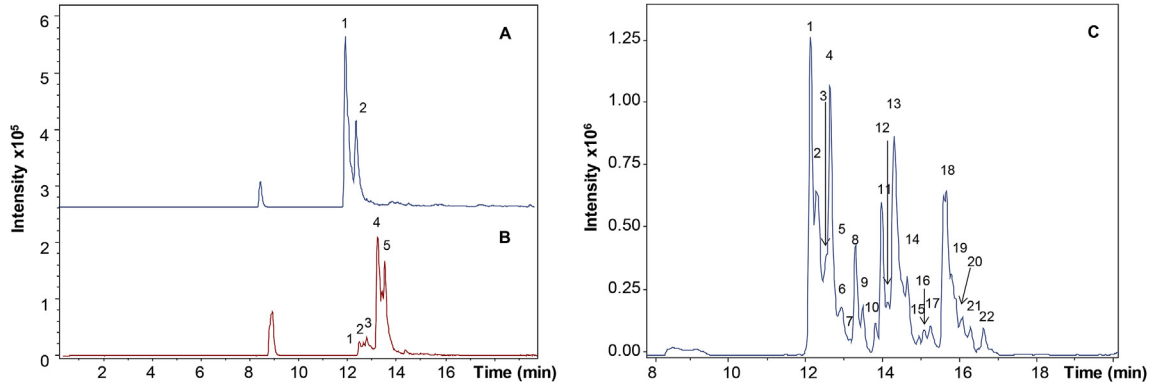


Fig. 1. Base-peak electropherograms obtained during low-flow sheathless CE-MS of samples of the nanobodies Nb1 (A), Nb1-35 GS-Nb1 (B) and Nb2 (C). Conditions: injected concentration, 1.0 μM (A, B) or 1.7 μM (C); BGE, 50 mM acetic acid (pH 3.0); separation voltage, 30 kV; pressure at capillary inlet, 0.5 psi; capillary temperature, 20 °C. Further conditions, see Experimental section.

Table 1
Assignment of species observed during low-flow sheathless CE-MS of Nb1 and Nb1-35 GS-Nb1.

peak[a]	observed mass (Da)	theoretical mass (Da)	assignment[b]	Δ mass (Da)
Nb1				
1	14590.97	14591.18	Nb1	0.21
2	14591.90	14592.17	deam Nb1	0.27
Nb1-35 GS-Nb1				
1	14590.72	14591.18	Nb1	0.46
2	14591.69	14592.17	deam Nb1	0.48
3	15527.70	–	not assigned	–
4	28835.74	28836.66	Nb1-35 GS-Nb1	0.92
5	28836.82	28837.65	deam Nb1-35 GS-Nb1	0.83

[a] Peak numbering according Fig. 1A (Nb1) and 1B (Nb1-35 GS-Nb1).
[b] Deam, deamidated.

Table 2
Assignment of species observed during low-flow sheathless CE-MS of Nb2.

peak[a]	observed mass (Da)	theoretical mass (Da)	assignment[b]	Δ mass (Da)
1	1639.79	1640.61	E129-H142	0.82
2	15498.58	15499.16	Nb2	0.58
3	15499.57	15500.15	1-deam Nb2	0.58
4	1953.47	1954.05	L126-H142	0.58
5	15499.55	15500.15	1-deam Nb2	0.60
	1640.79	1641.58	1-deam E129-H142	0.79
6	15500.54	15501.16	2-deam Nb2	0.62
7	15500.54	15501.16	2-deam Nb2	0.62
8	1640.78	1641.61	1-deam E129-H142	0.83
9	1954.53	1955.04	1-deam 126-H142	0.51
10	15087.41	15087.76	Nb2 – (H140-H142)	0.35
11	1953.98	1955.04	1-deam L126-H142	0.82
12	15088.30	15088.75	1-deam Nb2 –(H140-H142)	0.45
13	13562.69	13563.15	Nb2 – (L126-H142)	0.45
14	13875.88	13876.54	Nb2 – (E129-H142)	0.66
15	14004.94	14005.66	Nb2 – (E130-H142)	0.72
16	13305.97	13306.84	Nb2 – (Q124-H142)	0.87
17	13434.50	13434.97	Nb2 – (K125-H142)	0.47
18	14604.39	14605.26	Nb2 – (A136-H142)	0.87
19	14605.38	14606.25	1-deam Nb2 – (A136-H142)	0.87
20	14605.39	14606.25	1-deam Nb2 – (A136-H142)	0.86
21	14606.38	14607.24	2-deam Nb2 – (A136-H142)	0.86
22	14606.38	14607.24	2-deam Nb2 – (A136-H142)	0.86

[a] Peak numbering according Fig. 2B.
[b] 1-deam, singly deamidated; 2-deam, doubly deamidated.

the mass of native Myc-6xHis tag fragment. Based on the recorded mass spectra (Fig. 2A bottom), the two subsequent peaks (deconvoluted mass, 1640.79 and 1640.78 Da, respectively) both were assigned to singly deamidated forms of E130-H142. As the Myc-6xHis peptide fragment contains only a single asparagine residue (N133) and no glutamines, we speculate that the two observed isomers correspond to aspartic acid and iso-aspartic acid variants, which can be separated with CE [27].

For the full nanobody Nb2, two singly and two doubly deamidated species were observed, as could be concluded from the observed mass spectra obtained from the partially separated peaks (Fig. 2B). Again, CE showed its ability to separate isomeric protein variants, which in case of Nb2 may result from different positions of deamidation, as it comprises multiple asparagine residues. Overall, good sensitivity was obtained, allowing full characterization of the nanobodies, including variants and degradation products, upon injection of 1-μM samples (*i.e.* about 5 fmol of protein injected).

3.3. Profiling of mAbs

3.3.1. Intact mAbs

Monoclonal antibodies (mAbs) are complex molecules which show high heterogeneity. To ensure product quality and consistency, efficient analytical methods are needed to monitor variants related to e.g. C-terminal lysines, N-terminal pyroglutamate formation, deamidation, and glycosylation, as well as clipped species. Most mAbs are based on IgGs which contain one N-glycosylation site at N297 of the heavy chain (HC), leading to potentially two glycans per mAb molecule. This glycan decoration has a major impact on the biological function of the protein and also affects protein stability, solubility, antigenicity, folding and serum half-life [28,29]. Therefore, the glycosylation state is considered a critical quality attribute. The mAbs trastuzumab and ustekinumab were selected to explore the performance of low-flow sheathless CE-MS for intact mAb characterization.

As BGE, various concentrations of acetic acid were evaluated in terms of proteoform resolution and signal intensity. Addition of isopropanol to the BGE did not improve resolution of variants. Using 10% acetic acid, good signal intensity and mass spectral quality were obtained. Under these conditions, the trastuzumab sample showed a broad major peak, followed by two much smaller peaks (Figs. S3A and S4A). The deconvoluted spectrum of the main peak indicated a mixture of trastuzumab glycoforms that could be assigned mainly to non-sialylated fucosylated diantenary species (Fig. S3C). All observed glycoforms for trastuzumab exhibited a loss of a C-terminal lysine (K-clip). Moreover, species with masses between 146 and 147 kDa were detected, which were assigned to trastuzumab with only one glycan (Fig. S3C). Notably, fully non-

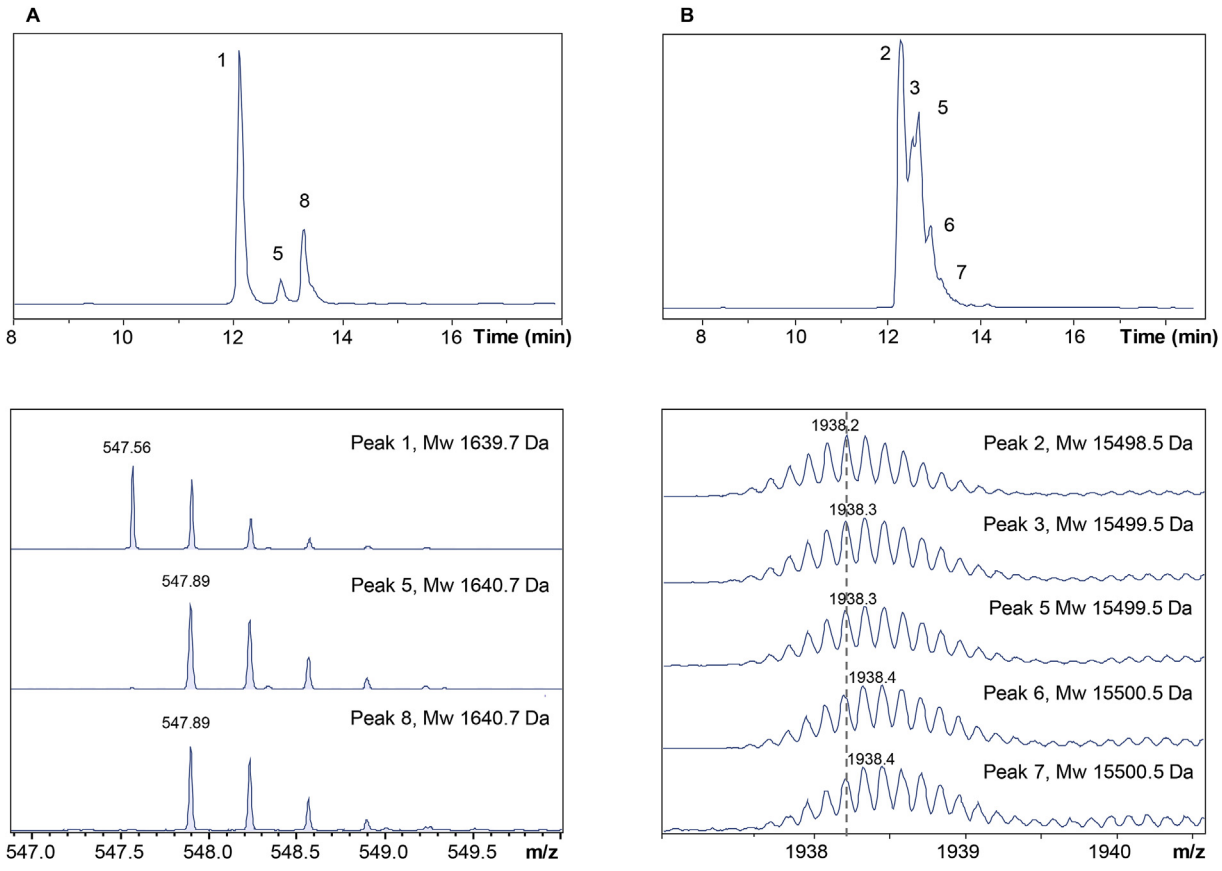


Fig. 2. Extracted electropherograms (top) and mass spectra (bottom) obtained during low-flow sheathless CE-MS of sample of nanobody Nb2. Conditions: extracted *m/z* range, 547.9 ± 0.5 (A) and 1938.2 ± 0.5 (B). Further conditions, see Fig. 1.

glycosylated species were not observed. Deconvolution of the mass spectrum obtained for the first minor peak (peak 2 in Fig. S4A), revealed a mass (23438.31 Da; Fig. S4B) that corresponds to a dissociated light chain of trastuzumab. These minor clipped forms can be difficult to determine without previous separation. Deconvolution of the mass spectrum obtained for the second minor peak (peak 3 in Fig. S4A) yielded the same mass as observed for the main peak. Based on the shift in migration time, we hypothesize that this peak corresponds to deamidated forms of trastuzumab, which are less positively charged than the native protein and, therefore, separated by CE. The mass change of the mAb induced by deamidation (+0.984 Da) which cannot be accurately measured by the mass spectrometer used.

Upon CE-MS analysis of ustekinumab, three partially separated peaks were observed (Fig. 3A), which appeared to consist of mixtures of variants (Fig. 3B). According the recorded masses, peak 1 mainly comprised non-sialated diantenary glycoforms with one C-terminal lysine. Peak 2 consisted mostly of K-clipped species containing one sialic acid in the glycan chain. Glycoforms containing more than two sialic acids (SiAs) were mostly observed in peak 3. SiA, in this particular case glycolylneuraminic acid (Neu5Gn) [30], reduces the overall pI of the protein resulting in its lower electrophoretic mobility. Considering the size of intact monoclonal antibodies (approximately 150 kDa) the charge contribution of one SiA to the total electrophoretic mobility is not sufficient to achieve baseline separation of the differently sialylated species. Migrating at 30.2 min, a small shoulder was discerned from peak 3. Deconvolution of the corresponding mass spectrum resulted in two low-abundant signals for the masses 74140 and 74301 Da, which correlate with the mass of a single light chain-heavy chain (LC-HC) containing a G0F or G1F glycan, respectively. These results illustrate the potential of sheathless CE-MS for the detection of native and clipped mAb forms and their major glycoforms.

3.3.2. *Middle-up analysis of mAbs*

The middle-up approach provides a practical alternative for intact protein analysis. In this approach, the protein of interest is cleaved to relatively large protein fragments (25–100 kDa) by reduction of the inter-chain disulphide bridges and/or using a specific protease. The use of the enzyme IdeS has become increasingly popular for the MS-based characterization of antibodies. IdeS cuts IgGs below the hinge region with high specificity, resulting in one F $(ab)_2$ fragment of about 100 kDa and two Fc/2 fragments of around 25 kDa.

In order to optimize the protein fragment and Fc/2 glycoform separation, the concentration acetic acid in the BGE was varied. Using a BGE of 50 mM acetic acid for the CE-MS analysis of IdeS-digested ustekinumab, only a single peak was observed. Deconvolution of the mass spectrum recorded for this peak revealed protein masses of about 25 and 100 kDa (corresponding to the Fc/2 and F $(ab)_2$ fragments, respectively), next to an unexpected protein mass of around 50 kDa. The latter was similar to the mass of to the full Fc fragment (two Fc/2 chains) (Fig. 4A). Increasing the acetic acid concentration in the BGE induced separation of the Fc/2 and F $(ab)_2$ fragments. At a concentration of 5% of acetic acid (Fig. 4B), the F $(ab)_2$ fragment was detected as a separate peak, whereas at later migration time two partially resolved peaks were observed. Based on their recorded masses, these could be assigned to Fc/2 and Fc fragments, respectively. Upon further increase of the acetic acid concentration to 10% (Fig. 4C), the mass corresponding to Fc was no

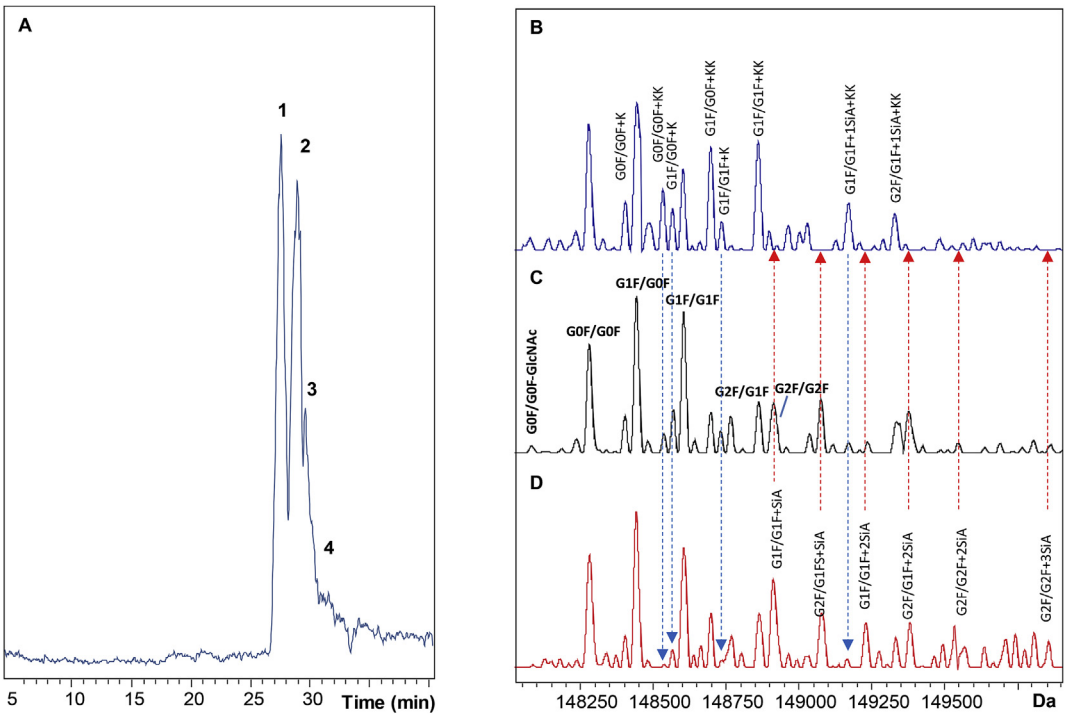


Fig. 3. Low-flow sheathless CE-MS of intact ustekinumab. (A) Base-peak electropherogram; (B–D) deconvoluted mass spectra obtained in apices of peaks 1, 2 and 3, respectively. Injected concentration, 0.5 μg/μL; BGE, 10% acetic acid; separation voltage 30 kV; pressure at capillary inlet 0.5 psi; capillary temperature, 20 °C. Further conditions, see Experimental section. Annotation: G0, core oligosaccharide containing four N-acetylglucosamines (GlcNAc) and three manoses (Man). G1 and G2, core oligosaccharide with one or two galactoses (Gal), respectively. S1 and S2, one or two sialic acids (N-Glycolyl neuraminic acid, Neu5Gc).

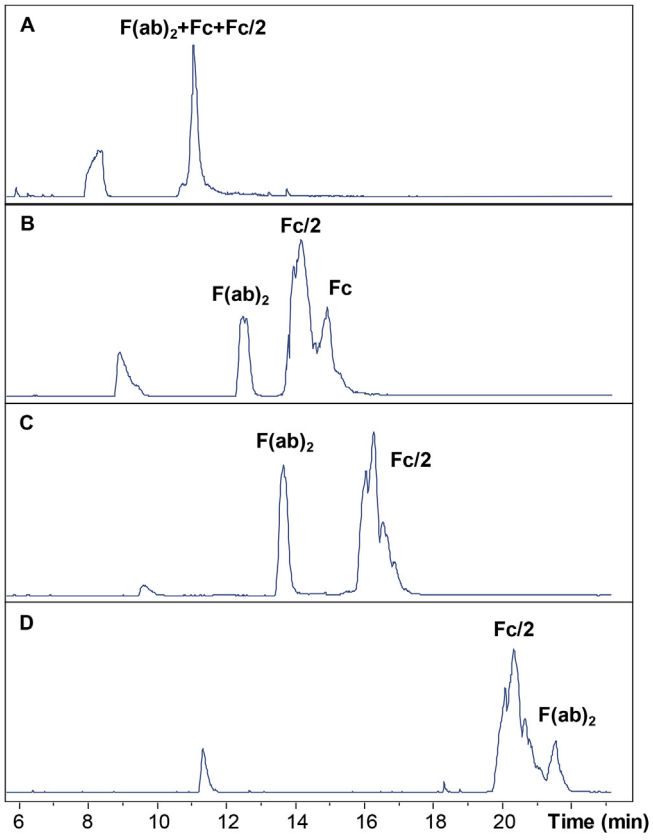


Fig. 4. Base-peak electropherograms obtained during low-flow sheathless CE-MS of IdeS-digested ustekinumab using (A) 50 mM acetic acid (pH 3.0), (B) 5% acetic acid, (C), 10% acetic acid, and (D) 20% acetic acid as BGE. Further conditions, see Fig. 3.

longer observed, but the Fc/2 band showed enhanced resolution, indicating partial separation of Fc variants. With respect to the Fc peaks, we speculate that the two Fc/2 fragments are still associated by non-covalent interactions at acetic acid concentrations below 10%. Higher concentrations of acetic acid apparently induce full dissociation of the Fc complex, resulting in only Fc/2 fragments in the electropherogram. As expected, protein migration times became longer with increasing acetic acid concentration. However, when the acetic acid concentration in the BGE was further increased from 10% to 20% (Fig. 4D), the F(ab)$_2$ fragment showed an increase of migration time from 14 min to 22 min, even leading to a swap in the migration order of the Fc and F(ab)$_2$ peaks. The same effect was observed when 10% of isopropanol was added to the BGE containing 10% acetic acid (Fig. S5). We hypothesize that the higher organic environment leads to (partial) unfolding of the F(ab)$_2$ fragment, decreasing its electrophoretic mobility. Therefore, 10% acetic acid was selected as optimum for the analysis of ustekinumab.

A complete characterization of the different Fc/2 variants observed under the optimized conditions is presented in Table 3. In addition to glycan and C-term Lys variability, Fc fragments containing other modifications, such as deamidation, were observed. Illustrating the separation power obtained with low-flow sheathless CE-MS, Fig. 5 shows some representative EIEs for Fc/2 variants. Separation appeared to be mainly driven by the differences in charged groups such e.g. lysine, aspartic acid, and sialic acid residues, whereas other structural variations in the glycan showed little contribution to the protein separation. Loss of a C-terminal lysine or addition of sialic acid to a glycan caused a shift to longer migration times, resulting in a Fc/2 peak resolution of about 1.0. Deamidation of asparagine in the Fc/2 chain caused a more substantial change of electrophoretic mobility, leading to a resolution of more than 3.0 from the non-deamidated species. This is in line

Table 3
Fc/2 PTM and glycoform assignment after low-flow sheathless CE-MS of ustekinumab.

migration time (min)	observed mass (Da)	theoretical mass (Da)	assigned PTM	Assigned glycan	Δ mass (Da)
15.50	23883.58	23883.04	–	non-glycosylated	−0.54
15.70	23755.02	23755.04	Fc/2-Kclip	non-glycosylated	0.02
15.90	25124.37	25125.14	–	G0F-NA	0.77
16.00	25327.46	25328.34	–	G0F	0.88
16.00	25181.52	25182.24	–	G0	0.72
16.00	25344.40	25344.14	–	G1	−0.26
16.00	25489.62	25490.54	–	G1F	0.92
16.10	25505.81	25506.54	–	G2	0.73
16.10	25652.05	25652.64	–	G2F	0.59
16.30	25814.18	25814.74	–	G2F+αGal	0.56
16.20	24996.87	24997.14	Fc/2-Kclip	G0F-NA	0.27
16.20	25200.27	25200.34	Fc/2-Kclip	G0F	0.07
16.20	25053.53	25054.24	Fc/2-Kclip	G0	0.71
16.30	25215.91	25216.14	Fc/2-Kclip	G1	0.23
16.30	25361.75	25362.54	Fc/2-Kclip	G1F	0.79
16.30	25378.51	25378.54	Fc/2-Kclip	G2	0.03
16.30	25524.32	25524.64	Fc/2-Kclip	G2F	0.32
16.40	25685.86	25686.74	Fc/2-Kclip	G2F+αGal	0.88
16.40	25650.62	25651.39	–	G1S1	0.77
16.40	25796.87	25797.79	–	G1FS1	0.92
16.40	25812.95	25813.79	–	G2S1	0.84
16.40	25959.32	25959.89	–	G2FS1	0.57
16.50	26121.25	26121.99	–	G2FS+αGal	0.74
16.40	25523.02	25523.39	Fc/2-Kclip	G1S1	0.37
16.60	25668.85	25669.79	Fc/2-Kclip	G1FS1	0.94
16.70	25831.24	25831.89	Fc/2-Kclip	G2FS1	0.65
16.70	25993.75	25993.99	Fc/2-Kclip	G2FS+αGal	0.24
16.50	26120.62	26121.04	–	G2S2	0.42
16.60	26266.65	26267.14	–	G2FS2	0.49
16.70	25993.02	25993.04	Fc/2-Kclip	G2S2	0.02
16.90	26138.77	26139.14	Fc/2-Kclip	G2FS2	0.37
17.00	25329.70	25329.32	deam	G0F	−0.38
17.20	25491.94	25491.52	deam	G1F	−0.42
17.20	25654.11	25653.62	deam	G2F	−0.49
17.40	25201.11	25201.32	Kclip + deam	G0F	0.21
17.40	25362.79	25363.52	Kclip + deam	G1F	0.73

Annotation: G0, core oligosaccharide containing four N-acetylglucosamines (GlcNAc) and three manoses (Man); G1 and G2, core oligosaccharide with one or two galactoses (Gal), respectively. S1 and S2, one or two sialic acids (N-Glycolyl neuraminic acid, Neu5Gc); Kclip, loss of C-terminal Lys; deam, deamidation.

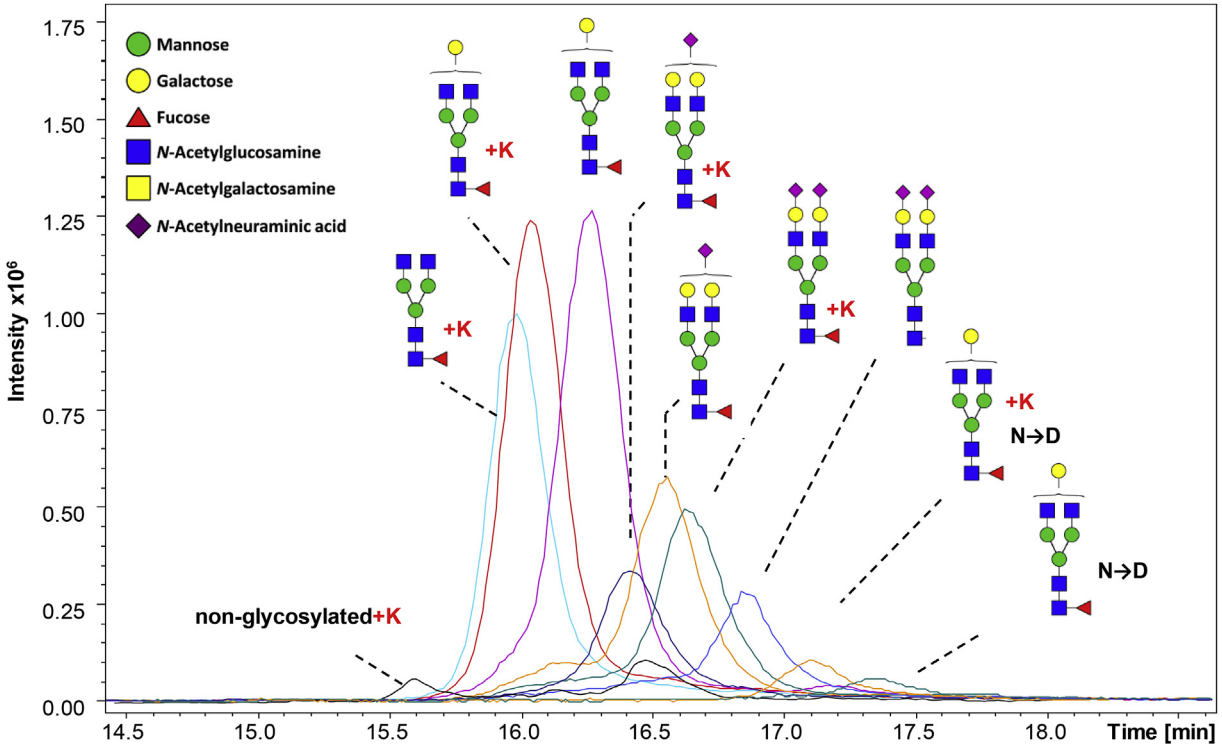


Fig. 5. Selected extracted-ion electropherograms obtained during low-flow sheathless CE-MS of IdeS-digested ustekinumab using a BGE of 10% acetic acid. Further conditions, see Fig. 3.

with the observed previously for other proteins by low flow sheathless CE-MS [31]. Non-glycosylated Fc/2 fragments exhibited a faster electrophoretic mobility compared to their glycosylated counterparts, probably as consequence of their lower hydrodynamic volume. Notably, no non-glycosylated species were observed during the CE-MS analysis of intact ustekinumab, indicating the complementarity of the intact and middle-up approach for assessment of antibody heterogeneity. Overall, low-flow sheathless CE-MS allowed assignment of 36 Fc/2 variants for ustekinumab (Table 3) underlining the usefulness of efficient separation and sensitivity for the characterization of minor variants.

In order to further evaluate the applicability of the low-flow sheathless CE-MS method for the characterization of mAbs, IdeS-digesed trastuzumab and infliximab were also analyzed. Fig. 6 provides the base-peak electropherograms for the three studies mAbs using a BGE of 10% acetic acid. Interestingly, the F $(ab)_2$ fragments of the respective mAbs show very different CE migration times under the applied conditions, whereas the migration times of the Fc/2 fragments are fairly similar. This can be explained by the fact that the F $(ab)_2$ fragment includes the most variable region of mAbs, and therefore provides more amino acid sequence variance and thus pI differences, which affect CE migration. The amino acid sequence of the Fc part is more conserved and mobility differences mainly originate from PTMs. In the case of the F $(ab)_2$ fragment of ustekinumab, trastuzumab and infliximab the migration time strongly increased as the percentage of acetic acid in the BGE is increased. At 5% acetic acid, the F $(ab)_2$ fragments of all tested mAbs migrated before their Fc/2 fragment, whereas at 20% acetic acid the F $(ab)_2$ migrated after the Fc/2 (Fig. S6).

The Fc/2 bands of the three mAbs clearly showed different profiles, which could be dissected by interpretation of the obtained mass information (Tables 3, S1 and S2). On average, the respective mAbs showed a different Fc/2 charge heterogeneity. Trastuzumab comprised only C-terminal-lysine-clipped variants and showed less glycan heterogeneity. Both infliximab and ustekinumab exhibited C-terminal lysine variability, and ustekinumab showed a high abundance of sialylated species. Glycoforms containing terminal SiA (Neu5Ac and Neu5Gln for trastuzumab and infliximab, respectively) were observed as low abundant species. These low-abundant species have not been reported in previous middle-up analysis of the same mAbs by LC-MS most probably due to their low abundance [32]. Regarding deamidation, the relative level of deamidation (*e.g.* ~10% for G1F, relative peak area) was higher for trastuzumab, when compared to ustekinumab (~2%) and infliximab (~0.5%). Determination of this modification would not have been possible without prior separation from the non-deamidated forms. Clearly, the low-flow sheathless CE-MS method facilitates both efficient separation of protein variants and sensitive detection, providing highly detailed Fc profiles using a middle-up approach.

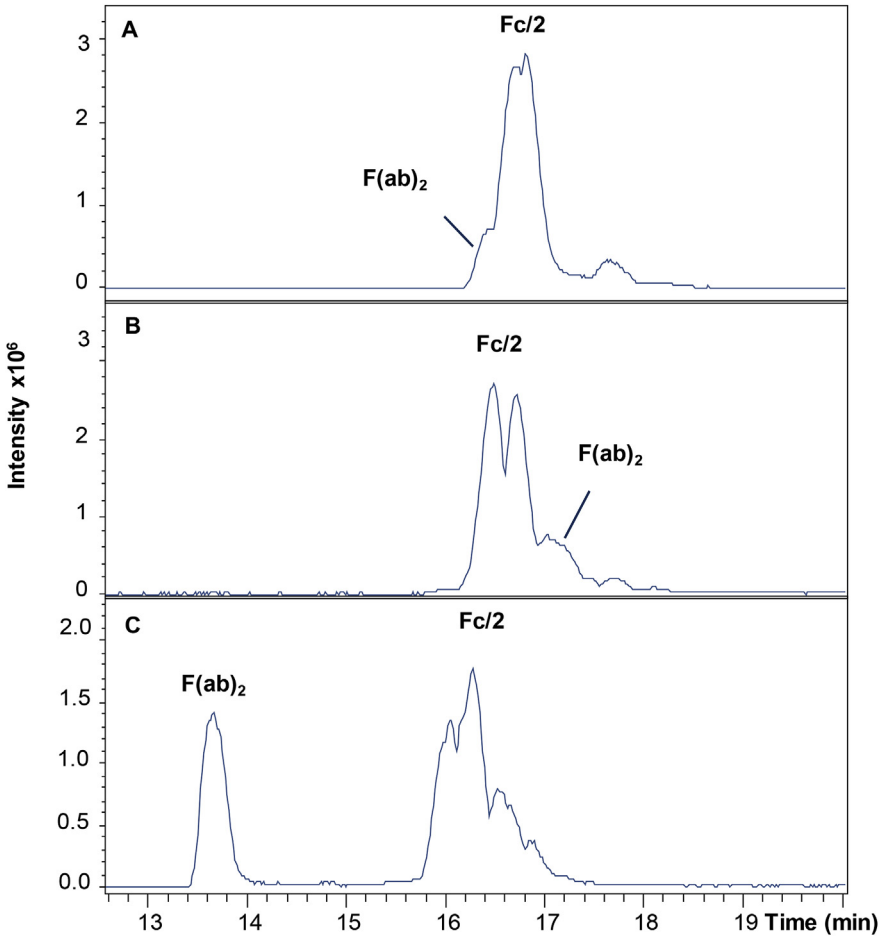


Fig. 6. Base-peak electropherograms obtained during low-flow sheathless CE-MS of IdeS-digested (A) trastuzumab, (B) infliximab and (C) ustekinumab. Injected mAb concentration, 0.5 μg/μL; BGE, 10% acetic acid. Further conditions, see Fig. 3.

4. Conclusions

In this work, we studied the usefulness of low-flow sheathless CE-MS for the characterization of antibody-based proteins. A commercial neutrally-coated capillary with a porous tip was used to avoid protein adsorption and to achieve a near-zero electroosmotic flow. This facilitated optimum protein separation and sensitive MS detection employing nanospray conditions. The CE-MS system showed great utility for the assessment of the purity and stability of nanobodies allowing assignment of deamidated, clipped and truncated forms. Moreover, the high resolving power provided separation of isomeric nanobody variants and fragments. Low-flow sheathless CE-MS of intact mAbs demonstrated to be useful for the assessment of macro-heterogeneity, revealing singly glycosylated and clipped forms, such as LC-HC fragments. Following a middle-up approach involving Ides digestion, high resolution of Fc charge variants and glycoforms was achieved for three different mAbs. Up to 32 Fc variants could be discerned per mAb from the detailed CE-MS profiles, indicating the potential of the method for assessment of mAb microheterogeneity. Overall, the electrophoretic mobility of the Fc/2 fragments of the respective mAbs was quite similar, whereas the mobility of the F $(ab)_2$ fragment appeared mAb specific. Moreover, the migration time of the F $(ab)_2$ fragment showed a strong dependency on the concentration acetic acid in the BGE, most probably due to protein conformational changes.

Acknowledgements

Authors would like to thank Marcia Santos, Stephen Lock and Jeff Chapman from Sciex for fruitful discussions and providing the prototype neutrally coated capillaries.

Appendix A. Supplementary data

Supplementary data related to this article can be found at https://doi.org/10.1016/j.aca.2018.08.024.

References

[1] G. Kohler, C. Milstein, Continuous cultures of fused cells secreting antibody of predefined specificity, Nature 256 (1975) 495–497.
[2] D.M. Ecker, S.D. Jones, H.L. Levine, The therapeutic monoclonal antibody market, Mabs-Austin 7 (2015) 9–14.
[3] P.M. Rudd, R.J. Leatherbarrow, T.W. Rademacher, R.A. Dwek, Diversification of the igg molecule by oligosaccharides, Mol. Immunol. 28 (1991) 1369–1378.
[4] S. Steeland, R.E. Vandenbroucke, C. Libert, Nanobodies as therapeutics: big opportunities for small antibodies, Drug Discov. Today 21 (2016) 1076–1113.
[5] A. Mujic-Delic, R.H. de Wit, F. Verkaar, M.J. Smit, GPCR-targeting nanobodies: attractive research tools, diagnostics, and therapeutics, Trends Pharmacol. Sci. 35 (2014) 247–255.
[6] R.H. de Wit, R. Heukers, H.J. Brink, A. Arsova, D. Maussang, P. Cutolo, B. Strubbe, H.F. Vischer, F. Bachelerie, M.J. Smit, CXCR4-Specific nanobodies as potential therapeutics for WHIM syndrome, J. Pharmacol. Exp. Therapeut. 363 (2017) 35–44.
[7] Z.Q. Zhang, H. Pan, X.Y. Chen, Mass spectrometry for structural characterization of therapeutic antibodies, Mass Spectrom. Rev. 28 (2009) 147–176.
[8] C.A.S. Barnes, A. Lim, Applications of mass spectrometry for the structural characterization of recombinant protein pharmaceuticals, Mass Spectrom. Rev. 26 (2007) 370–388.
[9] D. Ayoub, W. Jabs, A. Resemann, W. Evers, C. Evans, L. Main, C. Baessmann, E. Wagner-Rousset, D. Suckau, A. Beck, Correct primary structure assessment and extensive glyco-profiling of cetuximab by a combination of intact, middle-up, middle-down and bottom-up ESI and MALDI mass spectrometry techniques, mAbs 5 (2013) 699–710.
[10] A. Staub, D. Guillarme, J. Schappler, J.L. Veuthey, S. Rudaz, Intact protein analysis in the biopharmaceutical field, J. Pharmaceut. Biomed. 55 (2011) 810–822.
[11] K. Sandra, I. Vandenheede, P. Sandra, Modern chromatographic and mass spectrometric techniques for protein biopharmaceutical characterization, J. Chromatogr. A 1335 (2014) 81–103.
[12] R. Haselberg, G.J. de Jong, G.W. Somsen, Low-flow sheathless capillary electrophoresis-mass spectrometry for sensitive glycoform profiling of intact pharmaceutical proteins, Anal. Chem. 85 (2013) 2289–2296.
[13] M. Dawod, N.E. Arvin, R.T. Kennedy, Recent advances in protein analysis by capillary and microchip electrophoresis, Analyst 142 (2017) 1847–1866.
[14] S. Stepanova, V. Kasicka, Recent applications of capillary electromigration methods to separation and analysis of proteins, Anal. Chim. Acta 933 (2016) 23–42.
[15] A.L. Marie, E. Dominguez-Vega, F. Saller, J.L. Plantier, R. Urbain, D. Borgel, N.T. Tran, G.W. Somsen, M. Taverna, Characterization of conformers and dimers of antithrombin by capillary electrophoresis-quadrupole-time-of-flight mass spectrometry, Anal. Chim. Acta 947 (2016) 58–65.
[16] D.R. Bush, L. Zang, A.M. Belov, A.R. Ivanov, B.L. Karger, High resolution CZE-MS quantitative characterization of intact biopharmaceutical proteins: proteoforms of interferon-beta1, Anal. Chem. 88 (2016) 1138–1146.
[17] E.A. Redman, N.G. Batz, J.S. Mellors, J.M. Ramsey, Integrated microfluidic capillary electrophoresis-electrospray ionization devices with online MS detection for the separation and characterization of intact monoclonal antibody variants, Anal. Chem. 87 (2015) 2264–2272.
[18] E.A. Redman, J.S. Mellors, J.A. Starkey, J.M. Ramsey, Characterization of intact antibody drug conjugate variants using microfluidic capillary electrophoresis-mass spectrometry, Anal. Chem. 88 (2016) 2220–2226.
[19] J. Huhner, K. Jooss, C. Neusubb, Interference-free mass spectrometric detection of capillary isoelectric focused proteins, including charge variants of a model monoclonal antibody, Electrophoresis 38 (2017) 914–921.
[20] K. Jooss, J. Huhner, S. Kiessig, B. Moritz, C. Neususs, Two-dimensional capillary zone electrophoresis-mass spectrometry for the characterization of intact monoclonal antibody charge variants, including deamidation products, Anal. Bioanal. Chem. 409 (2017) 6057–6067.
[21] R. Haselberg, S. Oliveira, R. van der Meel, G.W. Somsen, G.J. de Jong, Capillary electrophoresis-based assessment of nanobody affinity and purity, Anal. Chim. Acta 818 (2014) 1–6.
[22] R. Heukers, I. Altintas, S. Raghoenath, E. De Zan, R. Pepermans, R.C. Roovers, R. Haselberg, W.E. Hennink, R.M. Schiffelers, R.J. Kok, P.M.P.V.B.E. Henegouwen, Targeting hepatocyte growth factor receptor (Met) positive tumor cells using internalizing nanobody-decorated albumin nanoparticles, Biomaterials 35 (2014) 601–610.
[23] Y.M. Zhao, L.L. Sun, M.D. Knierman, N.J. Dovichi, Fast separation and analysis of reduced monoclonal antibodies with capillary zone electrophoresis coupled to mass spectrometry, Talanta 148 (2016) 529–533.
[24] M. Han, B.M. Rock, J.T. Pearson, D.A. Rock, Intact mass analysis of monoclonal antibodies by capillary electrophoresis-Mass spectrometry, J. Chromatogr. B-Anal. Technol. Biomed. Life Sci. 1011 (2016) 24–32.
[25] D. Maussang, A. Mujic-Delic, F.J. Descamps, C. Stortelers, P. Vanlandschoot, M. Stigter-van Walsum, H.F. Vischer, M. van Roy, M. Vosjan, M. Gonzalez-Pajuelo, G.A.M.S. van Dongen, P. Merchiers, P. van Rompaey, M.J. Smit, Llama-derived single variable domains (nanobodies) directed against chemokine receptor CXCR7 reduce head and neck cancer cell growth in vivo, J. Biol. Chem. 288 (2013) 29562–29572.
[26] S. Tengattini, E. Dominguez-Vega, C. Temporini, M. Terreni, G.W. Somsen, Monitoring antigenic protein integrity during glycoconjugate vaccine synthesis using capillary electrophoresis-mass spectrometry, Anal. Bioanal. Chem. 408 (2016) 6123–6132.
[27] K. Faserl, B. Sarg, V. Maurer, H.H. Lindner, Exploiting charge differences for the analysis of challenging post-translational modifications by capillary electrophoresis-mass spectrometry, J. Chromatogr. A 1498 (2017) 215–223.
[28] A.R. Costa, M.E. Rodrigues, M. Henriques, R. Oliveira, J. Azeredo, Glycosylation: impact, control and improvement during therapeutic protein production, Crit. Rev. Biotechnol. 34 (2014) 281–299.
[29] P. Hossler, S.F. Khattak, Z.J. Li, Optimal and consistent protein glycosylation in mammalian cell culture, Glycobiology 19 (2009) 936–949.
[30] C.F. Yu, K. Gao, L. Zhu, W.B. Wang, L. Wang, F. Zhang, C.Y. Liu, M. Li, M.R. Wormald, P.M. Rudd, J.Z. Wang, At least two Fc Neu5Gc residues of monoclonal antibodies are required for binding to anti-Neu5Gc antibody, Sci. Rep. 6 (2016).
[31] R. Haselberg, G.J. de Jong, G.W. Somsen, Low-flow sheathless capillary electrophoresis-mass spectrometry for sensitive glycoform profiling of intact pharmaceutical proteins, Anal. Chem. 85 (2013) 2289–2296.
[32] V. D'Atri, S. Fekete, A. Beck, M. Lauber, D. Guillarme, Hydrophilic interaction chromatography hyphenated with mass spectrometry: a powerful analytical tool for the comparison of originator and biosimilar therapeutic monoclonal antibodies at the middle-up level of analysis, Anal. Chem. 89 (2017) 2086–2092.